can see from Table I, which gives the values of the constants in Eqs. (1) and (2).

IV. CONCLUSIONS

In conclusion, the present results provide direct supporting evidence for both the Mitchell mechanism and the related kinetics of the trapping of photoliberated holes. The end result of this mechanism is the buildup of halogen molecules by means of the alternate condensation of photoliberated holes and of positive-ion vacancies, created by the expulsion of positive ions to interstitial positions. These halogen molecules, in the present case of volume effect, remain within the crystal.[20] They constitute the counterpart of the metallic silver specks obtainable by volume irradiation at room temperature by the (complementary) alternate condensation of photoliberated electrons and mobile silver ions.

[20] L. Bellomonte *et al.* (to be published).

In addition, the present results provide a new technique for the study of several types of many-body interactions (e.g., phonon-plasmon interaction, etc.) as a function of the number of conduction electrons in the dark. This new technique appears particularly promising because it allows the number of conduction electrons to be varied in *one and the same sample* at *constant temperature* (that is, in one well-defined dynamical situation of the crystal). The possibility of using the above results to make new devices should also be noted. In particular, one might hope that the permanent photoconductivity here discussed could be "erased" by infrared illumination. Work is in progress also in this direction.

ACKNOWLEDGMENTS

It is a pleasure to thank Professor M. U. Palma for several discussions, and G. Sgroi, P. I. and V. Greco for help with the low temperatures.

PHYSICAL REVIEW VOLUME 188, NUMBER 3 15 DECEMBER 1969

Computer Simulation of the Lattice Dynamics of Solids*

J. M. DICKEY
Brookhaven National Laboratory, Upton, New York 11973

AND

ARTHUR PASKIN
Queens College of The City University of New York, Flushing, New York
and
Brookhaven National Laboratory, Upton, New York 11973

(Received 1 August 1969)

Neutron-diffraction data on dispersion curves for the rare-gas solids has emphasized the need for an anharmonic treatment of lattice dynamics. The molecular-dynamic technique is a powerful way of examining the temperature and volume dependence of phonon properties, since anharmonicity is treated without approximation. Using a Lennard-Jones potential, classical calculations have been made, at different temperatures and volumes, of average phonon properties such as pressure and energy, correlations in velocity and position, frequency distribution of normal modes, and phonon-dispersion curves. The volume dependence of the frequency was used to test the Gruneisen approximation. The magnitude of fluctuations in temperature and in the various correlations were compared with theory. These calculations predict relatively large shifts in frequency at constant volume as the temperature is raised in the regime where the classical approximation is valid.

I. INTRODUCTION

NEUTRON-DIFFRACTION measurements have recently[1,2] yielded phonon-dispersion curves for rare-gas solids at different temperatures, with the volume held constant, as well as at different densities. High-precision measurements of this type may ultimately provide critical tests of empirical pair potentials, anharmonic effects and the possible need for 3-body potentials.[3] The ability to measure phonon frequencies at constant volume over a wide range of temperatures generates a need for an exact treatment of anharmonicity. As measurements are made at arbitrary densities anharmonic frequency shifts, as a function of lattice spacing, are required to make meaningful comparison of experimental data with theoretical calculations. Further, recent interest in the phonon properties of extremely thin films and surface effects demands a

* Work was performed under the auspices of the U. S. Atomic Energy Commission.

[1] W. B. Daniels, G. Shirane, B. C. Frazer, H. Umebayashi, and J. A. Leake, Phys. Rev. Letters **18**, 548 (1967).

[2] J. A. Leake, W. B. Daniels, J. Skalyo, Jr., B. C. Frazer, and G. Shirane, Phys. Rev. **181**, 1251 (1969).

[3] D. L. Losee and R. O. Simmons, Phys. Rev. Letters **18**, 451 (1967); Phys. Rev. **172**, 934 (1968); **172**, 944 (1968).

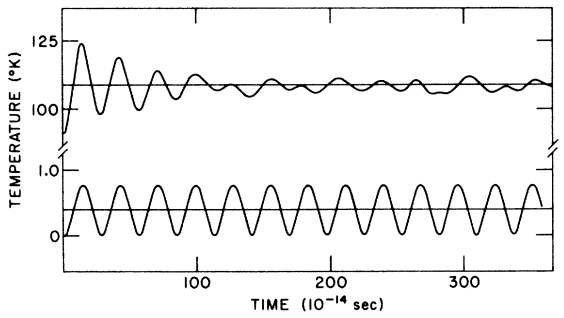

FIG. 1. Temperature response of the system to a perturbation in which the system is given, initially, additional potential energy in one mode. At high temperatures the energy is rapidly redistributed among all the modes, and at large times the fluctuations in temperature are commensurate with the number of atoms. At low temperatures the crystal behaves harmonically and there is no noticeable transfer of energy to other modes.

theoretical approach which does not rely on crystal symmetry.[4]

In recent years, there have been a number of calculations[5,6] for the rare-gas solids using a Lennard-Jones potential with empirical parameters and, for the most part, making the harmonic approximation. Anharmonicity has been tackled using various types of perturbation approaches[7]; e.g., the early terms in the perturbation series have been used.[8] Alternatively, the self-consistent phonon approach[9] is a partial summation of the even terms of the perturbation series. In addition most calculations have been made for the ideal Lennard-Jones interatomic spacing. In order to analyze experimental data at nonideal interatomic spacings and at high temperature and pressure, use is commonly made[1] of the Gruneisen relation between frequency and volume.

We shall here make use of the molecular-dynamic technique in calculating the lattice-dynamic properties of Lennard-Jones solids at a variety of volumes and temperatures. The advantage of this technique is that it allows us to treat the assumed interaction exactly without artifically decomposing it into harmonic and anharmonic contributions of various orders. We calculate the phonon-dispersion curves as a function of volume and temperature, and compare the volume dependence with the Gruneisen relationship. In the high-temperature region, the phonon lifetimes are calculated from the decay. The over-all phonon-frequency spectrum and useful thermodynamic quantities such as pressure and internal energy are also calculated, along with various particle correlations. The small number of particles used in the computer studies, emphasizes the role of fluctuations and allows quantitative comparison with fluctuation theory. We further show that the molecular-dynamic technique at low temperatures yields the results obtained analytically by Grindley and Howard[5] using the harmonic approximation. Using empirical constants appropriate for Ne and Kr, we compare the present classical calculation with observations. We attribute the negligible frequency shift observed in Ne as the temperature is raised at constant volume to the importance of the zero-point motion and the dominance of the low-frequency modes.

II. CALCULATIONS

Molecular-dynamic techniques as pioneered by Alder[10] have given considerable insight into the dynamics of solids and liquids. The basic procedure used in molecular-dynamic calculations, consists of solving Newton's equations in a difference form for a finite number of atoms, in this case 864. The explicit details of programming and the form chosen for the difference equation are given in the papers of Rahman[11] and Verlet,[12] which use molecular dynamics for calculating the properties of a Lennard-Jones fluid. There are many different ways of numerically solving Newton's differential equations of motion.

$$md^2\mathbf{r}_i/dt^2=\sum_{j\neq i}\mathbf{f}(r_{ij}), \tag{1}$$

where m is the mass, $\mathbf{r}_i$ is the position of the ith atom, and $f(r)$ is the force between two atoms distance r apart. In subsequent calculations the force will be derived from the Lennard-Jones potential

$$V(r)=\epsilon((\sigma/r)^{12}-2(\sigma/r)^6). \tag{2}$$

Results expressed in the natural units for the system (m, ϵ, $\sigma=1$) can be scaled to fit a particular substance by appropriate choice of these parameters. For concreteness, our results are presented in a form relevant to Kr, which because of its heavy mass, is well described by classical mechanics. The values for Kr of ϵ and σ have been taken from Grindley and Howard[5] and are 165.9°K and 4.13 Å, respectively.

By choosing a small time interval δ, the differential equations are approximated by difference equations of the following form

$$r_i(t+\delta)=r_i(t-\delta)+2r_i(t)+\sum_{j=i} f(r_{ij})\delta^2. \tag{3}$$

We chose this equation in preference to the predictor formula used by Rahman,[11] since the first iteration of the Rahman formula involves an extrapolated position

[4] J. M. Dickey and A. Paskin, Phys. Rev. Letters **21**, 1441 (1968); Bull. Am. Phys. Soc. **13**, 398 (1968).
[5] J. Grindley and R. Howard, in *Lattice Dynamics*, edited by R. F. Wallis (Pergamon Press, Inc., New York, 1965), p. 129.
[6] G. K. Horton and J. W. Leech, Proc. Phys. Soc. (London) **82**, 816 (1963).
[7] P. F. Choquard, *The Anharmonic Crystal* (W. A. Benjamin, Inc., New York, 1967).
[8] G. Leibfried, in *Lattice Dynamics*, edited by R. F. Wallis (Pergamon Press, Inc., New York, 1967), p. 237.
[9] N. S. Gillis, N. R. Werthamer, and T. R. Koehler, Phys. Rev. **165**, 951 (1968).
[10] B. J. Alder, J. Chem. Phys. **31**, 459 (1959).
[11] A. Rahman, Phys. Rev. **136**, A405 (1964).
[12] L. Verlet, Phys. Rev. **159**, 98 (1967).

based on earlier trajectories. In certain situations this artificially puts particles in regions of too-high-potential energy causing the iterative process to blow up. A small enough time interval must be chosen to assure both conservation of energy and minimization of cumulative errors arising from replacing the differential equations by difference equations. We have found that a time step of about 10^{-14} sec is adequate for the parameters appropriate to Kr, the random fluctuations in the total energy at high temperatures being of the order of 1 part in 10^{+5}.

In applying these techniques to simulate an infinite solid, periodic boundary conditions are used to eliminate surface effects. The atoms were arranged on an fcc lattice and brought into thermal equilibrium by several methods, depending on the temperature. For example, at low temperatures our system closely resembled a set of independent oscillators and the system could not, therefore, on its own attain equilibrium in practicable times. It was found that the initial distribution of energy among the modes persisted, and so the technique of initialization was critical. To simulate a classical system at constant temperature all modes should have equipartition of energy. A random-number table was used to generate random velocities at a series of times in the history of the system. The resultant energy of the system could be changed by scaling the velocities to obtain the desired temperature. This procedure was effective at high temperatures since anharmonic coupling does quickly redistribute energy among the modes, as was evident in the independence of the correlations on the exact method of preparation of a given temperature. The randomization-scaling procedure failed at low temperatures because of the system's harmonic behavior, which prohibited redistribution into the equilibrium state. The harmonic behavior at low temperatures was beautifully demonstrated when in the calculation of the dispersion curves the initialization was such that all the energy was concentrated in one mode which persisted *ad infinitum* (see Fig. 1). In order to treat the low-temperature case we had to average the results of several independent random initializations. The problem of initialization was much more difficult for a solid than in the earlier work on liquids because of the possibility of setting up, artificially, a nonequilibrium situation, which could persist over times long compared to the usual computer times.

After initialization, the system was allowed to come to its equilibrium values of temperature and pressure at the fixed volume. The temperature, pressure, and energy of the system were continuously monitored. The amplitude of vibrations, that is the mean square displacement of the atoms from their rest positions on the fcc lattice, was also monitored. The temperature θ was calculated from the average kinetic energy

$$\theta=(1/3N)\sum_i mv_i^2, \tag{4}$$

and the pressure P from the virial expression

$$P=\rho kT-(\rho/6N)\sum_{i,j>i} r_{ij}\cdot\partial v(r_{ij})/\partial r_{ij}, \tag{5}$$

where N is the total number of atoms in a volume V. The density ρ is N/V.

Equilibrium was determined by comparing the observed fluctuations[13,14] in temperature, and amplitude of vibrations, with calculated values. The fluctuations in temperature are given by the relationship[14]

$$\langle\Delta\theta^2\rangle_{\rm av}/\langle\theta\rangle_{\rm av}^2=2(1-3/2C)/3N. \tag{6}$$

In the harmonic limit, the specific heat $C=3$, so

$$\langle\Delta\theta^2\rangle_{\rm av}/\langle\theta\rangle_{\rm av}^2\approx 4\times10^{-4}, \tag{7}$$

for the number of particles under consideration. The system was considered in equilibrium when the fluctuations in temperature and mean-square amplitude were constant within 30% and were consistent with estimates of the equilibrium value. The technique of studying the fluctuations was sensitive enough to enable us to detect quickly the nonequilibrium aspects of our preliminary attempts at initialization at low temperature, e.g., if only one oscillator mode is populated the fluctuations in temperature are 0.5. Some sample average fluctuations, to demonstrate their variation over about 600 time steps, are 4.2, 3.4, 4.2, and 4.0×10^{-4}.

Having established that the system is in equilibrium, various thermodynamic properties were calculated. Figure 2 gives the variation with temperature at constant volume of the pressure, energy, and mean-square amplitude. The slope of the energy-temperature curve is the specific heat at constant volume, which, classically, is equal to $3k$ in the harmonic limit. The molecular-dynamic calculation gives the classical harmonic result, with a barely perceptible curvature at high temperatures resulting from anharmonicity. The effect of anharmonicity is more apparent from the pressure curve—for harmonic forces the pressure would be constant. The density was that for which an ideal Lennard-Jones solid would be in equilibrium at 0°K. Since the forces are treated only to second neighbor distances this gives a slight displacement in the absolute magnitude of the pressure and energy. The lattice constant was 5.67 Å. Using the melting curve given in Pollack[15] we would estimate the melting temperature of Kr at this density to be about 200°K. Most of our calculations were performed at three temperatures; a very low temperature of 2.51°K for which the harmonic approximation should be valid, a temperature of 186°K just below the estimated melting point, and a temperature of 91°K about half this value. Further calculations were performed at an expanded volume with a lattice constant of 5.80 Å,

[13] L. D. Landau and E. M. Lefschitz, *Statistical Physics* (Addison-Wesley Publishing Co., Inc., Reading, Mass., 1958).
[14] J. L. Lebowitz, J. K. Percus, and L. Verlet, Phys. Rev. **153**, 250 (1967).
[15] G. L. Pollack, Rev. Mod. Phys. **36**, 748 (1964).

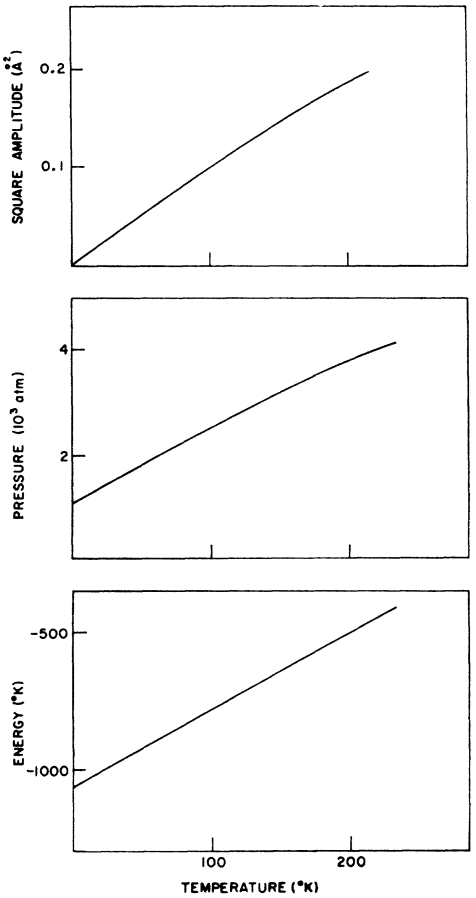

FIG. 2. Temperature dependence of the thermodynamic properties at a constant volume corresponding to a lattice parameter of 5.67 Å. Anharmonic effects show most clearly in the nonconstancy of the pressure.

for which the pressure was approximately zero. The compressibility was found from the data at these two different volumes to be 0.6×10^{-10} dyn cm^{-2}. Combining this value with the slope of the pressure-temperature curve gives a coefficient of expansion of 0.9×10^{-3} °K^{-1}. These values may be compared with experimental data for Kr provided one uses data from a high-temperature region where classical statistics obtain. At 80°K, the compressibility of Kr [15] is 0.5×10^{-10} dyn cm^{-2} and the coefficient of expansion is 1×10^{-3} °K^{-1}, which are very close to the values for our system. Using the Gruneisen equation of state,[16]

$$PV+V\partial U_0/\partial V=\gamma E_V, \tag{8}$$

where U_0 is the static potential energy, E_V is the vibrational energy, and the Gruneisen constant γ is 1.8. In Sec. III, this constant is determined more directly, from the phonon-dispersion curves, and is about 3.0 indicating an inconsistency in the simple Gruneisen equation of state.

[16] J. C. Slater, *Introduction to Chemical Physics* (McGraw-Hill Publishing Co., New York, 1939).

Having described how we initialize and calculate thermodynamic properties, it must be cautioned that such calculations are no more valid than the potential used to simulate the system. The Lennard-Jones potential is the most frequently used potential to approximate the properties of rare-gas solids. The advantage of the molecular dynamic technique is the ease with which any potential can be used. We have here used a Lennard-Jones potential because we can first check the reliability of the numerical techniques against more conventional calculations in the harmonic limit. As the phonon properties are sensitive to the derivatives of the potential, it is not surprising that parameters determined from other thermodynamic properties, usually in the gaseous state at high temperature, do not completely coincide with those chosen from essentially low-temperature solid-state properties. Therefore, in this work, we mainly emphasize changes in the lattice properties. We would expect that the use of better empirical potentials[15] would improve the agreement with experimental data. A further convenience to using the Lennard-Jones force is that in the fcc configuration there is a negligible contribution of 3rd- and higher-neighbor interactions. Therefore, only 1st- and 2nd-neighbor contributions were considered. Again, this is not a limitation of the technique as with the CDC 6600 used in these computations it would have been practicable to include as high as 5th-neighbor interactions.

III. AVERAGE PHONON PROPERTIES

Most earlier work on the thermal properties of solids has been concerned with such average properties as specific heat, Debye-Waller factor, thermal expansion, compressibility, distribution of normal modes, and zero-point motion. In order to test the accuracy of the molecular-dynamic technique, we have calculated classically several of these quantities at very low temperatures, where comparison can be made with the numerous calculations in the harmonic approximation. As many thermal properties can be expressed as moments of the phonon-frequency distribution, it is apparent that matching the frequency distribution implies that our method of calculation is as accurate as the exact harmonic treatments. Having established the accuracy of our technique, we then calculate similar properties at high temperatures to demonstrate the effects of anharmonicity.

The usual method of calculating the frequency spectrum involves finding the frequencies associated with a large number of wave vectors and using these to construct a histogram. In the molecular dynamic simulation of the motions in a system this information is contained implicity, and can be extracted by a suitable analysis of the correlations in the motion. For example, this can be demonstrated by analyzing the velocities of a collection of harmonic oscillators. Con-

sider a collection of classical harmonic oscillators with frequency distribution $f(\omega)$ analogous to a solid where each normal mode wave number $\mathbf{k}$ has a characteristic frequency ω, that is, $f(\omega)$ is the number of oscillators with frequency ω, normalized so that

$$\int f(\omega)d\omega=1. \tag{9}$$

For one oscillator, with amplitude A, phase φ, frequency ω

$$x=A\cos(\omega t+\varphi), \tag{10}$$

$$v=A\omega\sin(\omega t+\varphi), \tag{11}$$

where x is the position, v the velocity, m the mass, and the total energy is $mA^2/2\omega^2$. For a classical oscillator at temperature T,

$$mA^2\omega^2/2=kT. \tag{12}$$

The velocity correlation function $\gamma(t)$ is defined to be

$$\gamma(t)=\langle\sum v_i(t)\cdot v_i(0)\rangle/\langle\sum v_i^2(0)\rangle, \tag{13}$$

where the summation is over all the oscillators, and is averaged over a suitable ensemble. For the above collection,

$$\gamma(t)=\langle\sum A^2\omega^2\sin(\omega t+\varphi)\sin\varphi\rangle/\langle\sum A^2\omega^2\sin^2\varphi\rangle \tag{14}$$

$$=\langle\sum\sin(\omega t+\varphi)\sin\varphi\rangle/\langle\sum\sin^2\varphi\rangle, \tag{15}$$

using Eq. (11). If the averaging is over an ensemble with random phases φ, then

$$\langle\sin^2\varphi\rangle=\tfrac{1}{2},$$

$$\langle\sin(\omega t+\varphi)\sin\varphi\rangle=\tfrac{1}{2}\langle\cos\omega t-\cos(\omega t+2\varphi)\rangle=\tfrac{1}{2}\cos\omega t. \tag{16}$$

Hence,

$$\gamma(t)=N^{-1}\sum\cos\omega t. \tag{17}$$

Using the function $f(\omega)$ defined earlier and converting to an integral

$$\gamma(t)=\int f(\omega)\cos\omega t dt, \tag{18}$$

hence the Fourier transform of $\gamma(t)$ gives directly $f(\omega)$.

The velocity correlation $\gamma(t)$ that enters into $f(\omega)$ was obtained by approximating the ensemble averages by taking a series of different origins in the time evolution of a system—essentially invoking the ergodic hypothesis. In choosing the different time origins, the interval used was large enough so that most of the correlations with the previous time origin have disappeared. In Fig. 3, we show three typical velocity correlations at different temperatures. The time interval between origins corresponds to about 10^{-12} sec. The final average $\gamma(t)$'s, used in obtaining $f(\omega)$, were obtained using this procedure on a number of independently initialized systems. It might be noted that the top curve, corresponding to a low-temperature crystal, has

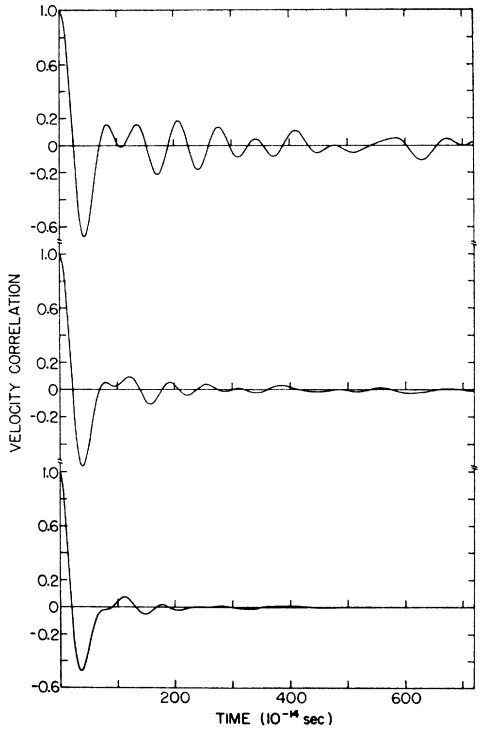

FIG. 3. Velocity autocorrelation at 2.51, 91, and 186°K, going from top to bottom. At low temperatures correlations persist for a number of vibrational periods, whereas at high temperatures the correlations rapidly disappear.

oscillations in the velocity correlation that persist for many vibrational periods, whereas the higher-temperature correlations vanish rapidly. We suspect that persistence of the oscillations at low temperature reflects the inadequacy of our statistical method. For an infinite Debye model, the asymptotic decay of $\gamma(t)$ [17] is $3(\omega_D t)^{-1}$, where ω_D is the Debye frequency. For the largest time value shown in Fig. 3, this would correspond to $\sim$0.04. From our definition of $\gamma(t)$ [Eq. (13)], it follows that the asymptotic fluctuations in γ are equal to the fluctuations in a velocity component. We estimate the asymptotic fluctuations of γ for a set of N harmonic oscillators to be of the order of $2(N)^{-1/2}$ $\sim$0.07. This is consistent with the low-temperature asymptotic behavior of $\gamma(t)$. For high temperatures, the phonons have a lifetime, and $\gamma(t)$ decays over some average lifetime, rapidly obliterating the statistical fluctuations.

To establish our accuracy, we compare in Fig. 4 the distribution of normal modes obtained by transforming $\gamma(t)$, for a Lennard-Jones potential with ideal lattice spacing, 1.37376σ, with the histogram derived by Grindley and Howard[5] using conventional harmonic analysis. The Grindley-Howard results are based on a sample of 108 000 points in the Brillouin zone, with the interaction extended to all neighbors. In the present

[17] B. R. A. Nijboer and A. Rahman, Physica 32, 415 (1966).

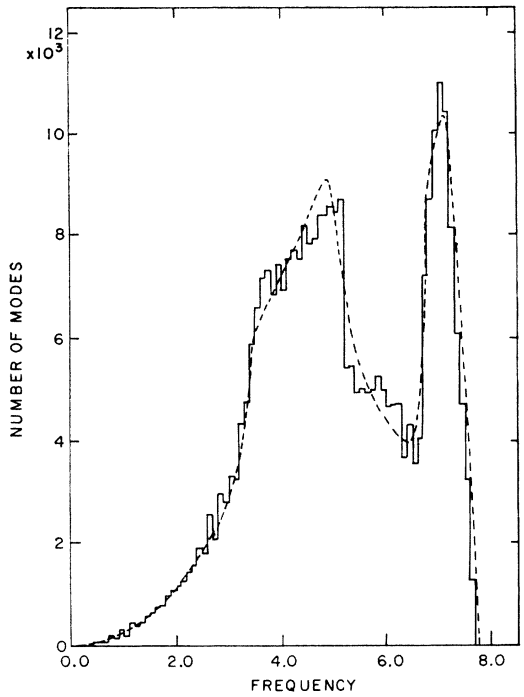

FIG. 4. Comparison of our frequency spectrum at low temperature (dashed curve) with the histogram of Grindley and Howard, based on the harmonic approximation. The units used are those adopted by Grindley and Howard.

calculation, we Fourier transform a velocity correlation for a finite interval of time. Because our $\gamma(t)$ is truncated, its Fourier transform has spurious ripples which we have smoothed out in the drawing. A combination of truncation errors and statistical fluctuations in our small sample would obscure sharp discontinuities. However, we do duplicate the major portion of the frequency distribution. The truncation limitation becomes less significant at high temperatures where anharmonicity smooths singularities. The effect of temperature is shown in Fig. 5 which shows how the frequency distribution is smeared in going from low temperature to high temperature at constant volume. Figure 5 clearly demonstrates that anharmonicity is important at high temperatures. The maxima of the transverse and longitudinal modes are shifted, as will subsequently be demonstrated more clearly in the dispersion curves, and the peaks are considerably washed out. At high temperatures the shape of the frequency distribution is smeared and looks more like the distribution of a liquidlike material.[11,18]

For comparisons with thermodynamic information it is more convenient to give the moments of the frequency distribution. As thermodynamic data is often quoted using Debye parameters, the moments are given in Table I in terms of the equivalent Debye frequency ω_D, rather than our computational units. For example, the zero-point energy equals $\frac{1}{2}\hbar\langle\omega\rangle$ and the zero-point amplitude equals $\hbar\langle\omega^{-1}\rangle/2m$. The low-temperature moments are well approximated by a Debye model, albeit the shape of $f(\omega)$ is clearly different. The very small change in the lower-order moments shows that the major change in $f(\omega)$ is broadening, rather than any systematic shift. This explains why corrections need not be made to zero-point properties at constant volume, although the finite amplitude of the zero-point motion does bring in anharmonicity. One further sees that the large excursions at high temperature mainly serve to broaden the frequency spectrum, whereas the main

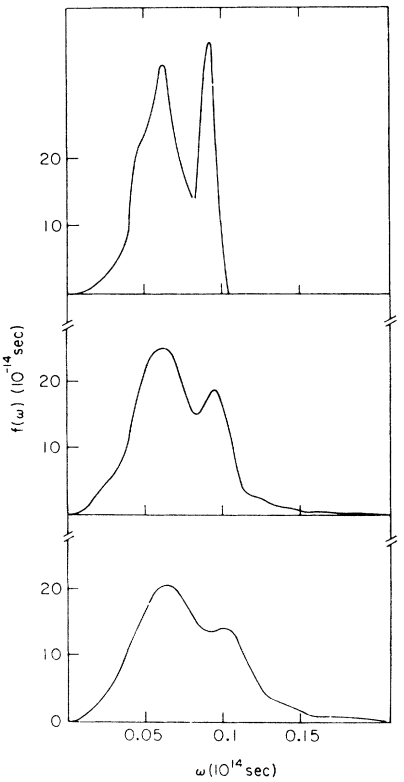

FIG. 5. Phonon-frequency spectrum at 2.51, 91, and 186°K, going from top to bottom. The broadening and frequency shifts at high temperature are evident. The high-temperature smoothing would remove any singularities.

TABLE I. Temperature and volume dependence of moments of the frequency distribution expressed in terms of the equivalent Debye frequency. The last row contains the average Gruneisen constant deduced from the first and fourth rows.

Lattice constant Å	Temperature °K	Equivalent Debye ω in 10^{14} sec $\langle\omega^2\rangle$	$\langle\omega\rangle$	$\langle\omega^{-1}\rangle$	$\langle\omega^{-2}\rangle$
5.67	2.51	0.089	0.088	0.088	0.094
	91	0.100	0.097	0.093	0.094
	186	0.108	0.103	0.096	0.096
5.80	2.52	0.073	0.073	0.074	0.078
γ	1.8[a]	3.1	2.9	2.7	2.9

[a] Value from the Gruneisen equation of state.

[18] A. Paskin, Advan. Phys. 16, 223 (1967).

effect of volume change is to change the average forces and thereby shift the frequencies. This explains the paradox of why the quasiharmonic approximation works so well in a crystal with a large degree of anharmonicity.

Figure 6 shows $f(\omega)$ at low temperatures for two different volumes, in the lower diagram the lattice parameter is expanded by about 2%. The frequency shifts are apparent and can be used to calculate a Gruneisen parameter. An average Gruneisen parameter γ is

$$\gamma = dln\omega_D/dlnV\,, \tag{19}$$

and is listed in the bottom row of Table I. The explicit frequency dependence of the Gruneisen parameter is examined subsequently. We have not calculated $f(\omega)$ for a series of volumes since a number have been published in the quasiharmonic approximation[19] and further a good approximation to $f(\omega)$ at different volumes can be obtained using the Gruneisen relation.

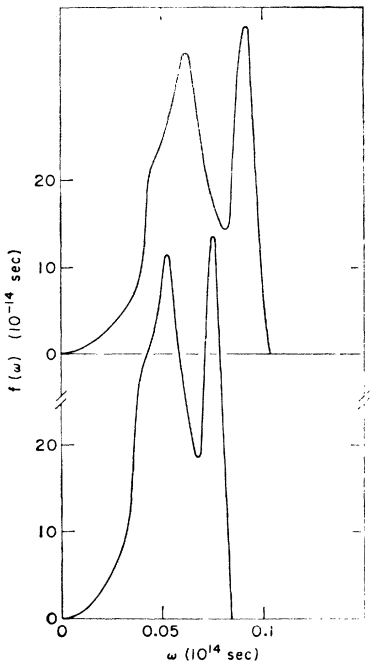

FIG. 6. Phonon-frequency spectrum at a low temperature but at two different volumes corresponding to lattice constants of 5.67 and 5.80 Å, for the upper and lower curves, respectively. In contrast to Fig. 5 the shape is not changed to first approximation.

We have discussed fluctuations in some correlations and average phonon properties. In certain instances the fluctuations can be related to frequency moments. Fluctuations in the mean-square amplitude of vibration illustrate this point. The mean-square amplitude α is

$$\alpha = \sum_i (r_i(t) - l_i)^2/N\,, \tag{20}$$

where r_i is the position of the ith atom and l_i the appropriate lattice site, and is familiar from its appearance in the Debye-Waller factor. Its temperature dependence is illustrated in Fig. 2. The slope of the square amplitude gives directly the value of $\langle 1/\omega^2\rangle$ listed in Table I. Its frequency dependence suggests that fluctuations in α should likewise depend on moments of the frequency. An explicit evaluation of $\langle \Delta\alpha^2\rangle_{av}$ in terms of temperature fluctuations yields the relation

$$\langle \Delta\alpha^2\rangle_{av}/\langle\alpha^2\rangle_{av} = (\langle \Delta\theta^2\rangle_{av}/\langle\theta^2\rangle_{av}) \cdot \langle\omega^{-4}\rangle/\langle\omega^{-2}\rangle^2. \tag{21}$$

Thus, it is not surprising that the fluctuations in α differ from the fluctuations in temperature. The difficulty in estimating this ratio of the moments is apparent from a consideration of the continuum Debye model where the average $\langle\omega^{-4}\rangle$ is divergent. However by replacing the numerator by a sum, and the denominator by a Debye model, we estimate the ratio to be about 2 for our system. The observed fluctuations range about 2–4 times the temperature fluctuations, but no detailed comparison could be made because of poor statistics. With good statistics the moment-dependent fluctuations would seem to be an interesting area for further study both theoretically and experimentally.

The position autocorrelation $\beta(t)$ is defined as

$$\beta(t) = \langle \sum_i (r_i(t) - r_i(0))^2/N\rangle/2\langle\alpha\rangle_{av}. \tag{22}$$

The normalization is chosen so that $\beta(t)$ asymptopically

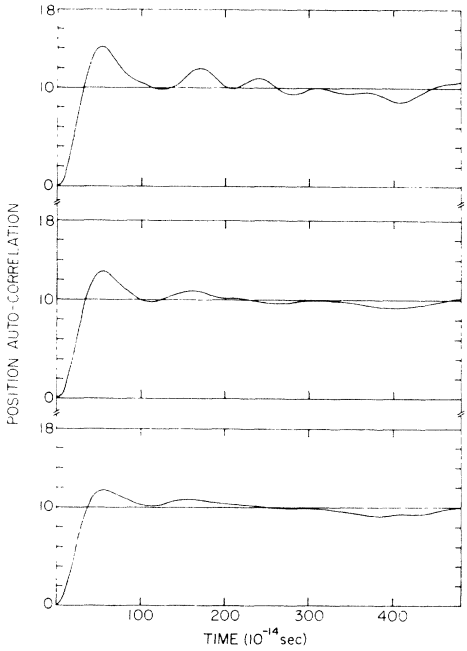

FIG. 7. Position autocorrelation at 2.51, 91, and 186°K going from top to bottom. At low temperatures correlations persist for a number of vibrational periods, whereas at high temperatures the correlations rapidly disappear.

[19] B. R. A. Nijboer and F. W. deWette, Phys. Letters **17**, 256 (1965).

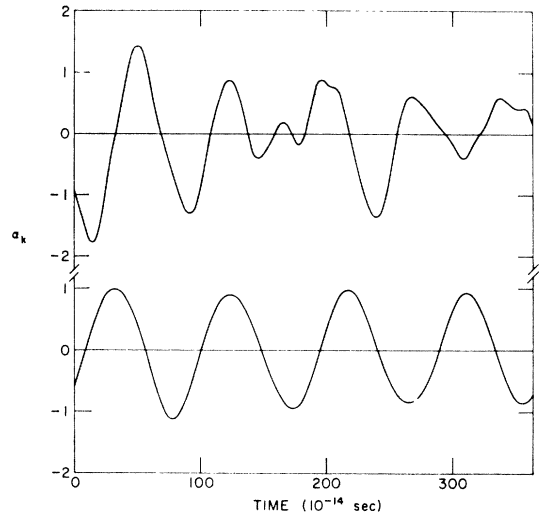

FIG. 8. Time evolution of a normal coordinate. The lower curve, corresponding to a low temperature, is approximately harmonic; this shows the independence of the phonons and justifies the harmonic approximation. At high temperature, upper curve, the motion is no longer harmonic, and energy is transferred to and from the mode.

goes to unity for large large time. The temperature variation of β is illustrated in Fig. 7. The averaging was performed in the same manner as for the velocity correlation. This correlation is of interest in that an asymptotic nonzero slope would indicate self-diffusion. In contrast to the behavior of the velocity correlation, one sees that fluctuations in β are less temperature-dependent over the same time interval. For large times, such that the positions at t and 0 are uncorrelated,

$$\beta(t) \rightarrow \langle \alpha(t)+\alpha(0) \rangle / 2\langle \alpha \rangle_{\text{av}}. \tag{23}$$

For the small number n of origins used in calculating the average in Eq. (22) the asymptotic fluctuations in β are similar to those of α scaled by $n^{-1/2}$.

IV. DISPERSION CURVES

One of the advantages of the molecular-dynamic technique is the ease of extracting dispersion curves to compare with neutron-diffraction results. In principle, there are a number of ways of Fourier analyzing the atomic motions to find the frequency associated with a given wave vector. In the harmonic approximation the normal coordinates of a periodic crystal α_q are given by

$$\alpha_q = \sum_i \mathbf{r}_i \cdot \mathbf{e}_q \cos \mathbf{q}\, \mathbf{l}_i, \tag{24}$$

where $\mathbf{e}_q$ is the polarization and $\mathbf{l}_i$ is the lattice site, and their temporal evolution is simply

$$\alpha_q(t) = \alpha_q{}^0 \cos(\omega_q t + \varphi_q). \tag{25}$$

In Fig. 8, the time evolution of α_q in high- and low-temperature regions is illustrated. At low temperatures, the curve is similar to the sinusoidal form that would be expected in the harmonic approximation, showing that there is little mixing of frequencies, and the modes defined by Eq. (24) are nearly independent. It is thus possible to obtain easily the frequency associated with a given wave vector. At high temperatures, because of anharmonicity, the coordinates defined in Eq. (24) are not independent, and so Eq. (25) for the time dependence does not hold. At higher temperatures, one finds that the amplitude and frequencies are continuously changing as shown in Fig. 8. It would require a long run to obtain a statistically reliable frequency. In addition to the dispersion relation, one can also obtain the spectral line shape by Fourier analyzing a long run—the time required must be much greater than the lifetime, which makes this method impracticable.

A more convenient method was to introduce a small perturbation with a particular wave vector and examine the response of the system. The perturbation consists of

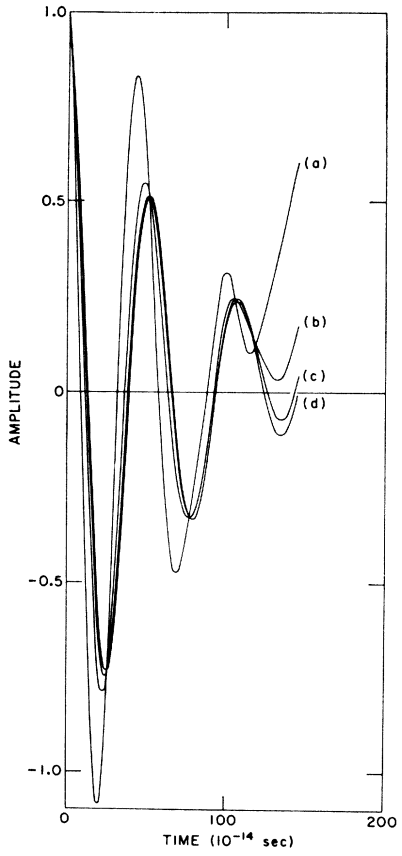

FIG. 9. Time evolution of a normal mode when, initially, excess energy has been concentrated in this mode. Curves (a), (b), (c), and (d) correspond to an excess energy of about 2, 5, 10, 20, respectively, times the ambient energy in the mode. All curves have been normalized to an initial value of unity. It can be seen that the frequency and the decay of the excess energy is independent of the magnitude of the initial perturbation provided that this is larger than the background noise. Curve (a) is directly comparable to the upper curve in Fig. 8 and the statistics are too poor for the frequency to be meaningful.

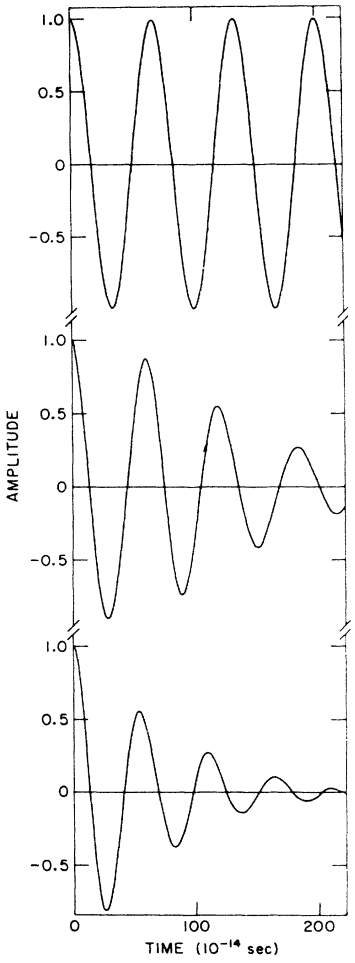

FIG. 10. Time evolution of a perturbed normal mode at 2.51, 91, and 186°K going from top to bottom. The shortening of the lifetime as the temperature is increased is evident.

modifying in a periodic way either the velocities or the positions of each atom in the solid. For example, if it is wished to introduce the perturbation as kinetic energy then in the difference equations at some time t the perturbed positions r' are defined by

$$r_i'(t)=r_i(t), \tag{26}$$

$$r_i'(t+\delta)=r_i(t+\delta)+\alpha_0 \cos q\cdot l_i, \tag{27}$$

and the system allowed to come to its new equilibrium. In the calculation of the dispersion curves, a constant additional amount of energy was introduced into the system each time by a suitable choice of α_0. The response of the system to this perturbation is shown in Fig. 1, which shows the kinetic energy alias temperature versus time. At low temperatures, the frequency response is sharp and the amplitude remains constant for long periods of time, whereas at a higher temperature, after a few initial oscillations, the disturbance disappears into the background noise. It is not possible to pick a frequency out of the temperature curve without causing a major change in the ambient temperature as shown in Fig. 1. Consequently, the perturbation technique, like the earlier analysis of the noise, is not practical at high temperatures.

By combining the two techniques of Fourier analysis and introducing a perturbation it is possible to get reliable frequencies in a reasonable amount of computer time, both at high and low temperatures using a small perturbation. As illustrated in Fig. 9 the decay of a mode is seen to be independent of the size of the disturbance. In this figure, different amounts of energy have been given but for comparison the amplitude has been normalized by dividing by the initial amplitude. From these curves, one can obtain not merely the frequencies but also the lifetimes associated with each mode. The constant α_0 was chosen at each temperature so that the disturbance could be distinguished from the background noise which is exactly the $\alpha_q(t)$ displayed in Fig. 8. Thus, the technique consists of introducing a disturbance small enough so there is a negligible change in temperature but large enough to be detected above the background noise. At 91°, α_0 was chosen to be about 8 times the background and at 186°, α_0 was chosen to be about 16 times the background. Typical curves for the decay of the excess energy in one mode due to its redistribution among other modes are shown in Fig. 10. It can be seen that a frequency can be obtained by following the motion for about 3–4 cycles. The calculation of the branches of the dispersion curves reported here, required about 2h of computer time.

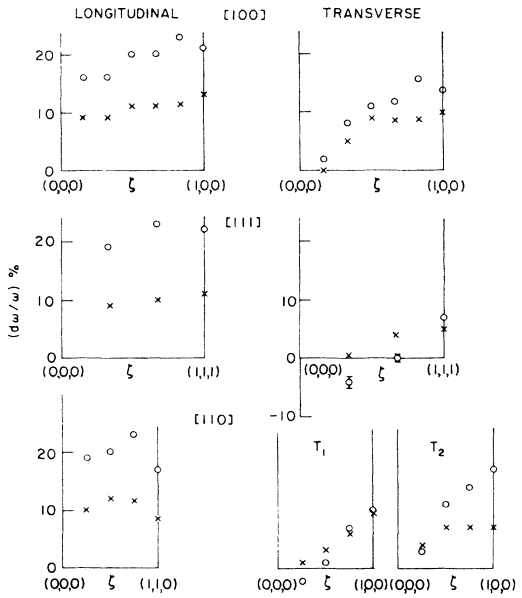

FIG. 11. Change in frequency at 91°, ×, and 186°, O, measured from the low-temperature values. The error is indicated by the bars in the transverse [111] modes. For the longitudinal modes the shifts are approximately wave-vector-independent, in contrast to the transverse modes. For the [110] transverse mode the two directions of polarization are $T_1=[1\bar{1}0]$ and $T_2=[001]$, and the frequency shifts differ for these two polarizations.

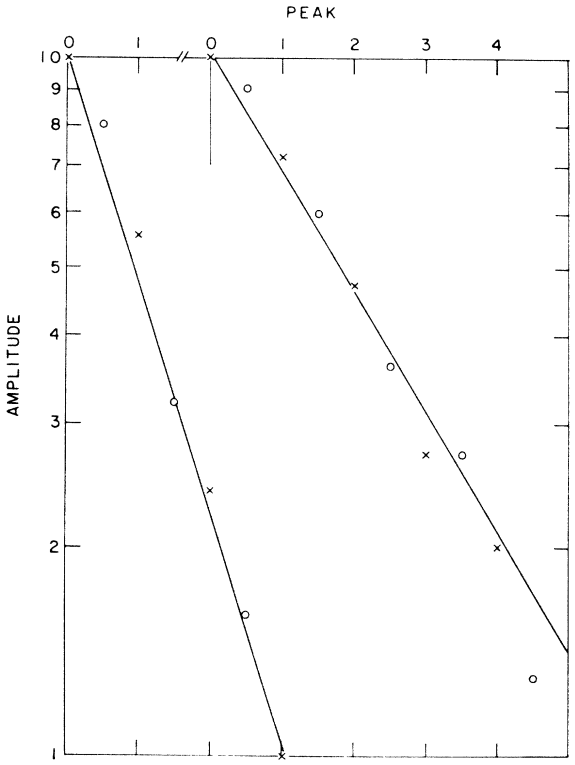

FIG. 12. Amplitude of successive peaks is plotted on a semilog scale, for a disturbance such as that shown in Fig. 10. The exponential decay of energy is apparent and the slope is a measure of the lifetime. The left-hand curve corresponds to a temperature of 186°K and the other curve to a temperature of 91°K.

At $\theta \sim 0°$, our frequencies are in agreement with the harmonic calculations of Grindley and Howard, which demonstrates the accuracy and reliability of our technique. Our results are identical to theirs within the accuracy of reading their figure so a dispersion curve at $\sim 0°$ is not repeated here. At high temperatures with their corresponding large excursions from equilibrium, the frequencies change even at constant volume, and the resultant frequency shifts are shown at two temperatures in Fig. 11. It might be noted that the frequency shifts are dependent on the mode, and in the case of the transverse, also on the wave vector and polarization. The frequencies of the longitudinal modes increase with increasing temperature and are relatively insensitive to wave vector. The transverse mode frequencies initially increase as the temperature is raised, but at the higher temperature, in some instances, the frequencies have decreased and may even fall below the zero-temperature values. This is in marked contrast to the longitudinal modes, where any systematic trends are barely discernible within the error, and we would estimate the average frequency shift for all modes to be about 0.1% per °K for Kr.

In Ne, it was observed[2] that there was a slight increase in the frequency (2.3±2.4%) for the longitudinal (100) mode. Our calculations qualitatively show the same trend as these experimental results. A simple physical argument can be made which explains these results. In the longitudinal mode, atoms come into contact with each other and the frequency of the mode mainly depends on an average of the steep repulsive part of the potential. As the temperature is increased the distance of closest approach of atoms decreases as the atoms sample the ever more steeply repulsive potential. This leads to a stiffening of the average force and an increase in the frequencies. For the transverse modes, the planes of atoms have sliding motions and sample less of the repulsive forces and more of the attractive forces. At higher temperatures, the fluctuations in position and the decrease in the effective size of the atoms tend to allow the atoms to more easily slide alongside of one another, and thus result in a lowering of the frequency associated with the transverse mode. Our results have been quoted in terms of parameters appropriate to Kr. In order to compare our classical system with the experimental results for Ne, care must be taken to take account of the effects of the quantum statistics on Ne. Since Ne has a small mass, it has a relatively large zero-point energy, and over the temperature range of the measurements of Daniels *et al.*, a large amount of the remaining energy is distributed over the low-frequency modes. For example, in these experiments, the temperature is raised from 4.7 to 25°K, which is about $\frac{1}{3}$ the Debye temperature, yet the total energy is increased only by about 20%. As the distance of closest approach of atoms is determined essentially by the energy stored in the system, we would expect that, for the longitudinal modes the anharmonic effects be proportional to the energy change. Scaling the previous figure for Kr, we would estimate a frequency shift for the longitudinal modes of Ne, at the two temperatures used, to be about $\frac{1}{5}$ the classical value, that is about 2%. The transverse modes depend less on the repulsive interaction and more on the attractive interaction. In a quantum system at low temperatures there is a larger relative proportion of transverse than longitudinal modes, because of the lower frequencies of the former. Thus one would expect that trends observed on our classical system, to be exaggerated in a quantum system. The decrease in the (100) mode observed for Ne is compatible with the softening trends observed in our classical system. It would be very interesting to see if our prediction of the softening trend increasing in the more closely packed directions is borne out by experiment.

Another consequence of the anharmonicity is the finite lifetime of the normal mode. At low temperatures, there is little anharmonicity and the amplitude of the perturbation is constant, Fig. 10; as the temperature is raised, the amplitude falls more rapidly. One can calculate a lifetime τ from the ratio of adjacent maxima A_1, A_2

$$A_1/A_2 = e^{-t/\tau}. \tag{28}$$

TABLE II. The Gruneisen constant for sample wave vectors.

Direction	ζ	Polarization	γ_k
[010]	$\frac{5}{6}$	L	3.1
[101]	$\frac{3}{4}$	T_2	2.9
[100]	$\frac{1}{3}$	T	2.8

The accuracy of an exponential decay is shown on Fig. 12 where the maxima are plotted on a log scale and are approximated by a straight line. At high temperatures the lifetime is of the order of a few oscillations. The lifetimes obtained in this manner do not depend on wave vector within the errors. So we quote the average lifetimes which are 0.23 and 0.55 periods, at 91° and 186°, respectively, scaled for Kr. These are much less than that observed for Ne. This may be attributed to the quantal behavior of Ne, but may also indicate the inaccuracy of the Lennard-Jones potential in the repulsive region, which determines the lifetimes. Our results are probably more reliable for changes rather then absolute values. It might be noted that such short lifetimes have been observed for some heavy metals (at high temperatures, e.g., Pb), and are not in themselves unreasonable.

In addition to the lifetimes, one could also get the spectral line shape, by Fourier analyzing the response to the perturbation. This involves a Fourier transform, which we find to be sensitive to truncation and the accuracy of the data at long times. In order to get reliable results, the computing time would be increased considerably. In Fig. 13, we show typical lines at two temperatures which complement the plot in Fig. 12. While the temperature broadening is demonstrated in the line shape the half-width is not exactly the same as that deduced from Fig. 12, because of truncation errors. We believe that the former technique is more reliable with the limited computing time available.

Since theoretical calculations of the dispersion curves are usually made at some fixed density, in order to compare with the experimental neutron-diffraction curves, which may be at a different density, the theoretical curves have been scaled using an empirical Gruneisen constant.[2] The Gruneisen constants γ_k are defined as

$$\gamma_k = \partial \ln \omega_k / \partial \ln V \tag{29}$$

and, in general, depend on the wave vector k. Two typical curves, to illustrate the dependence of frequency on volume, are shown in Fig. 14. It can be seen that the Gruneisen approximation is valid over volume changes up to about 8%. Sample values of γ_k are given in Table II which illustrates that γ_k is somewhat larger for larger wave vectors. An average value of γ can be found from the moments of the frequency spectrum, Table I. The value found from the higher-order moments, which weight the upper end of the frequency spectrum, are slightly larger than the γ found from $\langle \omega^{-1} \rangle$ which weights the lower frequencies. While γ_k does vary from mode to mode, use of an average γ is a good approximation in calculating a small correction. Other values of γ_k are not given here since values found using the quasiharmonic approximation[6,19] have been given elsewhere.

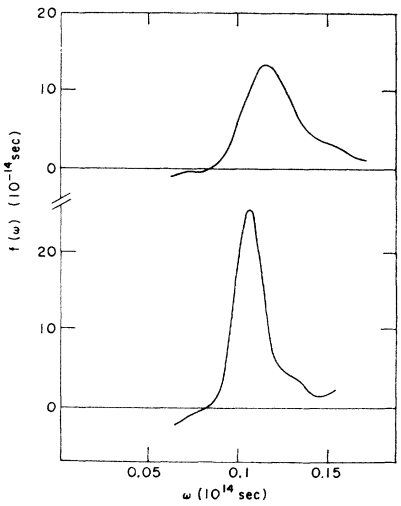

FIG. 13. Spectral line shapes obtained by Fourier transforming a disturbance similar to that shown in Fig. 10. The upper curve at 186°K has a greater width corresponding to a shorter lifetime than the lower curve at 90°K.

Having established the validity of using the Gruneisen relationship to convert phonon-dispersion curves to any desired density one can make use of the previous curves to compare with experimental data. Ideally, one uses the Lennard-Jones parameters, chosen to fit other thermodynamic properties, to scale the dispersion

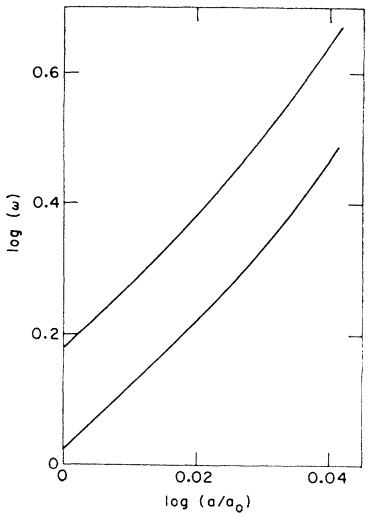

FIG. 14. Variation of frequency as the lattice is expanded at a low temperature. The upper curve corresponds to the [100] longitudinal mode and the lower curve to the [100] transverse mode. The curves are approximately linear near lattice spacing $=a_0$, the ideal Lennard-Jones spacing, showing the validity of using the Gruneisen approximation to scale each frequency with lattice spacing. (The base of the logarithms is 10.)

curves; then calculates the deviation of the real lattice parameter from the ideal Lennard-Jones lattice parameter, and uses the Gruneisen relation to find the consequent frequency shift. In the case of Kr, this procedure gives good agreement with experiment as previously shown by Daniels *et al.*[2] using the curves of Grindley and Howard. At the low temperature at which this experiment was performed, anharmonic effects are small and our calculations yield similar agreement. It is only at considerably higher temperatures that one could detect differences in the harmonic dispersion curves of Grindley and Howard, and the present calculations. Turning to Ne with its large zero-point properties one encounters a number of difficulties in choosing appropriate Lennard-Jones parameters. It is well known[20] that the parameters chosen in a classical approximation of a quantum property differ appreciably from parameters chosen from a quantum approximation. Therefore high-temperature (classical) Lennard-Jones parameters should not be expected to match low-temperature properties for a crystal with large quantum effects. Such inconsistencies in the Lennard-Jones parameters complicate the matching procedure and obscure the physical significance of comparing theory and experiment. Leake *et al.*[1] find a set of parameters which fall outside the range of high-temperature values, but do reproduce the Ne dispersion curves within experimental error. It would appear that one can find a Lennard-Jones parametric fit even to quantum systems such as Ne. But the physical significance of such a fit is lost, if the parameters do not, also, fit other unrelated properties. And so one should be cautious in applying the results of classical calculations like the present one to quantum systems such as Ne.

V. CONCLUSION

The present study using molecular-dynamic techniques to calculate phonon properties of solids may be analyzed in terms of the advantages and limitations of the technique, and the validity of the Lennard-Jones potential in describing rare gas or other solids.

The major advantage of our technique is that any force law may be treated exactly. As large-scale high-speed computers are now commonplace, it is possible to calculate (using reasonable computer times), phonon and thermodynamic properties of an assemblage of about 1000 atoms. Such calculations reproduce calculations made in the appropriate harmonic regions, and allow for extensions into high-temperature high-pressure regions, which have hitherto been inaccessible to theoretical calculations. The limitation of the calculation is that it is classical. Moreover, the use of periodic boundary conditions with a small number of particles excludes the study of phenomena dependent on large numbers of particles such as critical effects. Replacing the differential equations by difference equations requires the use of time steps, short compared to the frequency of vibration, thus computer studies are limited to phenomena whose relaxation time is less than about 1000 atomic vibrations.

In order to compare theory with experimental data one requires an accurate pair potential. For the rare-gas solids a Lennard-Jones potential is apparently a first approximation. There are a variety of more exact empirical potentials which can be used to explain the properties of rare gases from the gaseous to the solid state. As more exact measurements are made such potentials should be used. It is only by using the best empirical pair potentials that the need for a three-body potential can be assessed. The agreement of the Lennard-Jones potential with the data of Kr suggests that phonon properties will not require a three-body potential. Lennard-Jones potentials are reasonable approximations for classical properties of rare-gas solids. In addition, they may also be used to study relative phonon properties in metals, such as the dependence of frequency spectrum on geometry in thin films and small particles.[4]

[20] B. J. Alder and M. Van Thiel, Phys. Letters **7**, 317 (1963).